Chapter 2
Design by Testing and Statistical Determination of Capacity Models

Giorgio Monti, Antonio Bilotta, Annalisa Napoli, Emidio Nigro, Floriana Petrone and Roberto Realfonzo

Abstract In this chapter, the procedure proposed in EN1990 is adopted and extended to the case of EBR FRP systems, with the aim of attaining a uniform reliability level among all equations developed in this technical report. This approach will allow comparing experimental results and theoretical predictions in a consistent manner, and also identifying possible sources of error in the formulations. Any capacity model should be developed on the basis of theoretical considerations and subsequently fine-tuned through a regression analysis based on tests results. The validity of the model should then be checked by means of a statistical interpretation of all available test data. The formulation should include in the theoretical model a new variable that represents the model error. This variable is assumed to be normally distributed whit unit mean and standard deviation to be evaluated from comparison with experimental results. Once the statistical parameters of the model error are known, it is possible to define the statistical parameters of the capacity model and to evaluate its characteristic value, which is the aim for application in design. Some applications are shown to prove the feasibility of the proposed procedure.

Introduction

When developing a design equation, the predictive ability of the analytical capacity model, regardless of how it has been obtained, whether through a mechanics-based approach or through a regression from test data, must be validated over a reasonably large(r) set of experimental data. Thus, the definition of a reliable capacity

G. Monti (✉) · F. Petrone
Sapienza University of Rome, Rome, Italy
e-mail: giorgio.monti@uniroma1.it

A. Bilotta · E. Nigro
University of Naples Federico II, Naples, Italy

A. Napoli · R. Realfonzo
University of Salerno, Salerno, Italy

C. Pellegrino and J. Sena-Cruz (eds.), *Design Procedures for the Use of Composites in Strengthening of Reinforced Concrete Structures*, RILEM State-of-the-Art Reports 19, DOI 10.1007/978-94-017-7336-2_2

model to be used in practical design applications requires to follow a rigorous procedure that eventually will aim at calibrating the safety factor to apply to the equation so that it meets an assigned reliability target. This procedure requires the model to be formulated in a probabilistic way, so that both inherent and epistemic uncertainties of the underlying basic variables (geometry and materials, essentially) can be dealt with, as well as the uncertainties associated to the capacity equation itself. All of these uncertainties can be easily incorporated into a model, through the adoption of a random variable that represents the difference between actual and predicted response.

Probabilistic Capacity Models: Analytical Definition

As widely illustrated by Monti et al. (2009) (and also by Monti and Petrone 2014 who extended the procedure to the case of additive uncertainties), a capacity model should be defined as:

$$C\{f;a\} = R\{f;a\} \cdot \delta\{X_i\} \tag{2.1}$$

where: R is a function that "explains" the resisting mechanism capacity, given certain mechanical properties f and geometrical properties a, and represents the "deterministic" part of the capacity model; $\delta\{X_i\}$ is a random variable containing information about the overall model error prediction with respect to experimental results, and represents the "random" part of the capacity model. It is characterized by mean $\mu_\delta = b$ and variance σ_δ^2 and is a function of all the X_i parameters characterized by uncertainties. In the following it will be assumed: $\{X\}_i = \{f;a;m\}$, where f, a and m are parameters related to materials, geometry and model, respectively.

In common practice, only the deterministic part of the capacity model is considered, usually given as:

$$C_{\text{det}}\{f;a\} = b \cdot R\{f;a\} \tag{2.2}$$

Many interpret b as a model fine-tuning coefficient (sometimes called "ignorance" coefficient), so that, when the "deterministic" (mean) part of the capacity model is used, see Eq. (2.3), it predicts the experimental capacity with zero error "in the average". The coefficient b is computed through a least-square approach, by minimizing "in the average" the difference between predicted and experimental values. Pictorially speaking, the coefficient b brings the "cloud" of "theoretical-experimental" points closer to the bisectrix of the Cartesian plan.

Therefore, once the functional form $R\{f;a\}$ is found, in order to completely describe the random variable δ, we perform n experimental tests T, by "appropriately" changing the values of f and a. So, by selecting n sets of values $\{f_{\text{exp},i}; a_{\text{exp},i}\}$, we obtain n experimental values of the capacity, expressed as:

$$C = T\{f_{\text{exp},i}; a_{\text{exp},i}\} \cdot \tau \quad (i = 1 \ldots n) \tag{2.3}$$

where τ represents a random error, with unit mean and assigned variance, the latter being due to test setup imprecisions, load application modality, and measurement errors that may affect the results. Usually, this term is disregarded (in the sense that the measured values $C_{\text{exp},i}$ already include it).

The corresponding values predicted by the "deterministic" model are:

$$C_{\text{det},i}\{f_{\text{exp},i}; a_{\text{exp},i}\} = b \cdot R\{f_{\text{exp},i}; a_{\text{exp},i}\} \tag{2.4}$$

By comparison of n experimental and theoretical values, b is found from the well-known minimization:

$$\min \sum_{i=1}^{n} \left(\frac{C_{\text{exp},i}}{C_{\text{det},i}} - 1 \right)^2 \rightarrow b \tag{2.5}$$

Equation (2.7) can be analytically developed to finally obtain:

$$b = \frac{\sum_{i=1}^{n} \left(\frac{C_{\text{exp},i}}{R\{f_{\text{exp},i}; a_{\text{exp},i}\}} \right)^2}{\sum_{i=1}^{n} \frac{C_{\text{exp},i}}{R\{f_{\text{exp},i}; a_{\text{exp},i}\}}} \tag{2.6}$$

The variance of δ is obtained as well, as:

$$\sigma_{\delta}^2 = Var\left[\frac{C_{\text{exp}}}{C_{\text{det}}} \right] \tag{2.7}$$

with its unbiased estimate being (after b has been fine-tuned):

$$s_{\delta}^2 = \frac{\sum_{i=1}^{n} \left(\frac{C_{\text{exp},i}}{b \cdot R\{f_{\text{exp},i}; a_{\text{exp},i}\}} - 1 \right)^2}{n - 2} \tag{2.8}$$

By replacing Eq. (2.2) into Eq. (2.1), the following relation holds:

$$C\{f; a\} = C_{\text{det}}\{f; a\} \frac{\delta\{X_i\}}{b} \tag{2.9}$$

Letting:

$$\overline{\delta}\{X_i\} = \frac{\delta\{X_i\}}{b} \tag{2.10}$$

$\overline{\delta}\{X_i\}$ represents the model error to be applied to the fine-tuned deterministic capacity model. It is characterized by mean $\mu_\delta = 1$ and variance:

$$\sigma_{\overline{\delta}}^2 = \frac{1}{b^2} Var\left[\frac{C_{\exp}}{C_{\det}}\right] \tag{2.11}$$

with its estimate being (after b has been fine-tuned):

$$s_{\overline{\delta}}^2 = \frac{\sum_{i=1}^{n}\left(\frac{C_{\exp,i}\{f_{\exp,i};a_{\exp,i}\}}{b\cdot R\{f_{\exp,i};a_{\exp,i}\}} - 1\right)^2}{b^2(n-2)} \tag{2.12}$$

Calibration of Partial Safety Factors Based on Testing

Once the random part has been "adjusted" by means of experiments, a common, though wrong, further step is to use only the deterministic part to predict the capacity, with the assumption that its characteristic and design values can be obtained by plugging in the argument, respectively, characteristic and design values. Worse usual mistakes regard an arbitrary reduction of b, to obtain a "safer" estimate. In the following, a rigorous and effective procedure is instead developed, where the "modeling" part is clearly distinguished from the "safety" part.

The probabilistic capacity model so developed has first-order-approximation mean and variance given by, respectively:

$$\mu_C = b \cdot R\{\mu_f;\mu_a\} \cdot \mu_{\overline{\delta}} = b \cdot R\{\mu_f;\mu_a\} \tag{2.13}$$

$$\begin{aligned}\sigma_C^2 =& C_{,f}^2\{\mu_f;\mu_a\} \cdot \sigma_f^2 + C_{,a}^2\{\mu_f;\mu_a\} \cdot \sigma_a^2 + C_{,\overline{\delta}}^2\{\mu_f;\mu_a\} \cdot \sigma_{\overline{\delta}}^2 \\ =& b^2 \cdot R_{,f}^2\{\mu_f;\mu_a\} \cdot \sigma_f^2 + b^2 \cdot R_{,a}^2\{\mu_f;\mu_a\} \cdot \sigma_a^2 + b^2 \cdot R^2\{\mu_f;\mu_a\} \cdot \sigma_{\overline{\delta}}^2\end{aligned} \tag{2.14}$$

where $C_{,f} = \partial C/\partial f$, $C_{,a} = \partial C/\partial a$ and $C_{,\overline{\delta}} = \partial C/\partial\overline{\delta}$ are the partial derivatives of the function C with respect to f, a, and $\overline{\delta}$, respectively, and $R_{,f} = \partial R/\partial f$, $R_{,a} = \partial R/\partial a$ and $R_{,\overline{\delta}} = \partial R/\partial\overline{\delta}$ are the partial derivatives of the function R with respect to f, a, and $\overline{\delta}$, respectively. Also, note that all variables have been assumed as statistically independent, so that all covariance are zero.

In Eq. (2.14), the first term of the second member represents the intrinsic (material) uncertainty, the second term represents the parametric (geometry) variability, and the third term represents the epistemic (model) uncertainty.

Case of limited number of tests

When predicting a limited number of tests n, we can only obtain estimates of mean and variance of the capacity model, as follows:

$$C\{\overline{f};\bar{a}\} = b \cdot R\{\overline{f};\bar{a}\} \tag{2.15}$$

$$\begin{aligned} &s_C^2\{\overline{f};\bar{a}\} \\ &= b^2 \cdot R_{,f}^2\{\overline{f};\bar{a}\} \cdot s_f^2 + b^2 \cdot R_{,a}^2\{\overline{f};\bar{a}\} \cdot s_a^2 + b^2 \cdot R^2\{\overline{f};\bar{a}\} \cdot s_{\overline{\delta}}^2 \end{aligned} \tag{2.16}$$

where:

$$\overline{f} = \frac{\sum_{i=1}^{n} f_i}{n} \; ; \quad \bar{a} = \frac{\sum_{i=1}^{n} a_i}{n} \tag{2.17}$$

$$s_f^2 = \frac{\sum_{i=1}^{n} \left(f_i - \overline{f}\right)^2}{n-1} \; ; \quad s_a^2 = \frac{\sum_{i=1}^{n} (a_i - \bar{a})^2}{n-1} \tag{2.18}$$

and where $R_{,f} = \partial R/\partial f$, $R_{,a} = \partial R/\partial a$ and $R_{,\overline{\delta}} = \partial R/\partial \overline{\delta}$ are the partial derivatives of the function R with respect to f, a, and $\overline{\delta}$, respectively.

Under the hypothesis that C is normally distributed, when we have a limited number of tests, the characteristic value of the capacity model has a non-central t-Student distribution with n–1 degrees of freedom and with non-centrality parameter equal to $u_\alpha\sqrt{n}$ (notice that, when looking for the characteristic values in a normal distribution, which is the 5 % fractile, we have: $u_\alpha = 1.645$). An unbiased estimate (mean) of the characteristic value is (see e.g., Madsen et al. 1986):

$$C_k\{\overline{f};\bar{a}\} = C\{\overline{f};\bar{a}\} - k_{\alpha,n} \cdot s_C\{\overline{f};\bar{a}\} \tag{2.19}$$

where $k_{\alpha,n}$ is:

$$k_{\alpha,n} = u_\alpha \varepsilon_n = u_\alpha \sqrt{\frac{n-1}{2}} \frac{\Gamma\left(\frac{n-1}{2}\right)}{\Gamma\left(\frac{n}{2}\right)} \tag{2.20}$$

with Γ the Gamma function. An excellent approximation to the above equation is here proposed as:

$$k_{\alpha,n} = u_\alpha \varepsilon_n = u_\alpha \frac{4n-5}{4n-6} = u_\alpha \frac{n-1.25}{n-1.50} \tag{2.21}$$

For the purpose of the following developments, it is expedient to rewrite Eq. (2.19) as:

$$C_k\{\overline{f};\bar{a}\} = C\{\overline{f};\bar{a}\} - u_\alpha \varepsilon_n \cdot s_C\{\overline{f};\bar{a}\} \tag{2.22}$$

where ε_n becomes a sort of "scaling" coefficient of the capacity axis, easily determined for practical purposes as function of the number n of tests performed as:

$$\varepsilon_n = \frac{n - 1.25}{n - 1.50} \tag{2.23}$$

Having determined the characteristic value of the capacity model, the next step is the determination of its design value. This is given as:

$$C_d\{\overline{f};\bar{a}\} = \frac{C_k\{\overline{f};\bar{a}\}}{\gamma_C} = \frac{C\{\overline{f};\bar{a}\} - u_\alpha \varepsilon_n \cdot s_C\{\overline{f};\bar{a}\}}{\gamma_C} \tag{2.24}$$

where the safety factor γ_C is to be calibrated by considering that the design value is found as:

$$C_d\{\overline{f};\bar{a}\} = C\{\overline{f};\bar{a}\} - \beta_{LS}\alpha_C\varepsilon_n \cdot s_C\{\overline{f};\bar{a}\} \tag{2.25}$$

where it should be noted that the axis has been scaled by means of the same coefficient ε_n to account for the limited amount of tests; in the above equation, β_{LS} is the safety index associated to the acceptable exceeding probability of the considered Limit State in a given time period, and α_C is the FORM sensitivity coefficient associated to capacity variables.

Thus, the safety factor is found as:

$$\gamma_C = \frac{C_k\{\overline{f};\bar{a}\}}{C_d\{\overline{f};\bar{a}\}} = \frac{C\{\overline{f};\bar{a}\} - u_\alpha \varepsilon_n \cdot s_C\{\overline{f};\bar{a}\}}{C\{\overline{f};\bar{a}\} - \beta_{LS}\alpha_C\varepsilon_n \cdot s_C\{\overline{f};\bar{a}\}} \tag{2.26}$$

This is the factor that, once applied to the characteristic value $C_k\{\overline{f};\bar{a}\}$, gives the design value of the capacity model, $C_d\{\overline{f};\bar{a}\}$. Notice that there is an explicit dependence of the safety factor on the number of tests performed.

The above procedure needs now to be applied to the format adopted in Eurocode 0 (EN 1990) for all capacity equations, which reads as follows:

$$C_{d,EC0}\{f_d;\bar{a}\} = \frac{1}{\gamma_{Rd}} b \cdot R\{f_d;\bar{a}\} = \frac{1}{\gamma_{Rd}} b \cdot R\left\{\frac{f_k}{\gamma_m};\bar{a}\right\} \tag{2.27}$$

According to the Eurocode philosophy, safety factors are divided into "internal" ones, such as the different γ_m's, applied to material properties, and an "external" one, such as γ_{Rd}, applied to the capacity model. The former are meant to cover the intrinsic uncertainties in the material properties, while the latter deals with epistemic uncertainties related to the model. This format allows calibrating γ_{Rd} separately from the γ_m's, which may as well be taken as those already given in the code.

Thus, we should impose:

$$C_{d,EC0}\{f_d;\bar{a}\} = C_d\{\overline{f};\bar{a}\} \tag{2.28}$$

$$\frac{1}{\gamma_{Rd}} b \cdot R\left\{\frac{f_k}{\gamma_m}; \bar{a}\right\} = C\{\bar{f}; \bar{a}\} - \beta_{LS}\alpha_C \varepsilon_n \cdot s_C\{\bar{f}; \bar{a}\} \tag{2.29}$$

$$\begin{aligned} &\frac{1}{\gamma_{Rd}} R\left\{\frac{f_k}{\gamma_m}; \bar{a}\right\} \\ &= R\{\bar{f}; \bar{a}\} - \beta_{LS}\alpha_C \varepsilon_n \sqrt{R_{,f}^2\{\bar{f}; \bar{a}\} \cdot s_f^2 + R_{,a}^2\{\bar{f}; \bar{a}\} \cdot s_a^2 + R^2\{\bar{f}; \bar{a}\} \cdot s_{\bar{\delta}}^2} \end{aligned} \tag{2.30}$$

Finally, the sought general expression for the "external" safety factor accounting for the number of tests performed is found as:

$$\gamma_{Rd} = \frac{R\left\{\frac{f_k}{\gamma_m}; \bar{a}\right\}}{R\{\bar{f}; \bar{a}\} - \beta_{LS}\alpha_C \varepsilon_n \sqrt{R_{,f}^2\{\bar{f}; \bar{a}\} \cdot s_f^2 + R_{,a}^2\{\bar{f}; \bar{a}\} \cdot s_a^2 + R^2\{\bar{f}; \bar{a}\} \cdot s_{\bar{\delta}}^2}} \tag{2.31}$$

Notice that the safety factor depends on the number of tests performed through: ε_n, $\bar{f}$, $\bar{a}$, s_f^2, s_a^2, and $s_{\bar{\delta}}^2$, where the latter also contains the "ignorance" coefficient b, which represents a measure of the prediction capability of the capacity equation.

The above equation can be used to calibrate the "external" safety factor of any capacity equation, with a known functional form $R\{\cdot\}$, and with the "internal" safety factors already provided by the relevant code.

Also notice that, when dealing with quality-controlled materials, such as steel, one may replace the sample estimates $\bar{f}$ and s_f^2 with the corresponding population parameters μ_f and σ_f^2, so that the characteristic value of the material property may also be found as: $f_k = \mu_f - 1.645\sigma_f$. In this case, by knowing the coefficient of variation V_f, mean and variance can be easily found from the characteristic value as:

$$\mu_f = \frac{f_k}{1 - 1.645V_f} \tag{2.32}$$

$$\sigma_f^2 = \left(\frac{V_f f_k}{1 - 1.645V_f}\right)^2 \tag{2.33}$$

The safety factor then becomes:

$$\gamma_{Rd} = \frac{R\left\{\frac{f_k}{\gamma_m}; \bar{a}\right\}}{R\{\mu_f; \bar{a}\} - \beta_{LS}\alpha_C \varepsilon_n \sqrt{R_{,f}^2\{\mu_f; \bar{a}\} \cdot \sigma_f^2 + R_{,a}^2\{\mu_f; \bar{a}\} \cdot s_a^2 + R^2\{\mu_f; \bar{a}\} \cdot s_{\bar{\delta}}^2}} \tag{2.34}$$

Therefore, the design capacity is:

$$R_d\left\{\frac{f_k}{\gamma_m};\bar{a}\right\} = \frac{1}{\gamma_{Rd}} b \cdot R\left\{\frac{f_k}{\gamma_m};\bar{a}\right\} \tag{2.35}$$

Application 1—End Debonding

In this section, an application of the design by testing procedure is shown for the assessment of a design formulation to predict the end debonding load in Reinforced Concrete (RC) members strengthened with FRP Externally Bonded Reinforcement (EBR). Indeed, the high performances of FRP materials often cannot be properly exploited, since a typical failure is the debonding of the external reinforcement, namely the loss of bond at the concrete/FRP interface. This makes the bond strength at the interface a key issue in the strengthening design procedure. Usually debonding occurs within a thin layer of concrete and is related to its very low strength.

Several theoretical formulations have been proposed by researchers and international codes to predict the maximum stress in the FRP reinforcement when the end (Chen and Teng 2001; fib bulletin 2001; CNR-DT 200 2004; Smith and Teng 2002) or the intermediate debonding (Teng et al. 2003) occurs. Most of these formulations, characterized by similar structures, are calibrated by numerical factors based on experimental results.

Even though the assessment of models for bond strength has been widely dealt with by various researchers, the definition of safety factors to calculate design values is still an open item. Thus, detailed statistical analyses have been performed using a wide experimental database of bond tests in order to calibrate a bond strength model based on the fracture energy approach. The final proposed strength model is similar to other well-known models suggested in the literature and codes, but it is based on a detailed and consistent statistical analysis according to the 'design by testing' procedure suggested in the Eurocode 0 (Monti et al. 2009; Bilotta et al. 2011a; Monti and Petrone 2014). Different corrective factors allow both mean and characteristic values of debonding load to be predicted in order to follow a limit state design approach and associate a structural safety to the chosen model.

The approach to calculate the bond strength based on the fracture energy at the FRP-to-concrete interface has been summarized.

In order to develop statistical analyses, the experimental debonding loads of several bond tests have been collected and compared with three well-known relationships providing the end-debonding load in order to assess their reliability. Then, the same data have been used to assess a new relationship for the end-debonding-load according to the 'design by testing' procedure. In particular, numerical factors for both mean and percentiles provisions have been calibrated in order to furnish design provisions.

Moreover, the preformed and cured in situ EBR FRP systems have been distinguished to better exploit the performance of the latter ones.

Theoretical Formulations of Debonding Load

The maximum tensile force, $F_{\max}$, at debonding in an FRP external reinforcement characterized by an infinite bonded length can be calculated as:

$$F_{\max} = b_f \int_0^{\infty} \tau_b(x)dx \tag{2.36}$$

being $\tau_b(x)$ the bond shear stress distribution along the concrete-FRP interface and b_f the width of the FRP reinforcement.

Moreover, the fracture energy corresponding to a generic bond shear stress-slip law, $\tau_b(s)$, can be expressed as:

$$\Gamma_F = \int_0^{\infty} \tau_b(s)ds \,[\mathrm{F/L}] \tag{2.37}$$

This expression has the meaning of energy [FL] for unit surface [L^2].

Moreover, under the hypothesis that the concrete member has a stiffness much larger than the reinforcement, at the section in which the maximum stress, $\sigma_{f,max}$, is applied, the following relationship can be written:

$$\int_{A_f} \frac{1}{2} \cdot \sigma_f \cdot \varepsilon_f dA = b_f \cdot \int_0^{\infty} \tau_b(s)ds \tag{2.38}$$

This expression assumes the equality of the energy [F L] for unit length [L] associated to the tensile stress at the FRP section (area $A_f = b_f\, t_f$) with the fracture energy [F L] for unit length [L] developed at the FRP-concrete interface. Furthermore, assuming constant stresses along the FRP reinforcement section and a linear-elastic stress-strain relationship, Eq. (2.38) can be written as follows:

$$\frac{\sigma_f^2}{2 \cdot E_f} \cdot t_f \cdot b_f = b_f \cdot \Gamma_F \quad \frac{\left(\sigma_f \cdot t_f \cdot b_f\right)^2}{2 \cdot E_f} \cdot = b_f^2 \cdot t_f \cdot \Gamma_F \tag{2.39}$$

that gives the expression:

$$F_{\max} = b_f \cdot \sqrt{2 \cdot E_f \cdot t_f \cdot \Gamma_F} \tag{2.40}$$

where t_f, b_f, E_f are the thickness, the width, and the Young's modulus of the FRP reinforcement.

The fracture energy, Γ_F, depends on both the strength properties of adherents, concrete, and adhesive, and the characteristics of the concrete surface. If the FRP reinforcement is correctly applied, the debonding occurs in the concrete and the specific fracture energy of the interface law can be written in a form similar to that used for the shear fracture (Mode I). Therefore, the fracture energy can be expressed as a function of the concrete shear strength: $\Gamma_F(\tau_{b,max})$, where $\tau_{b,max}$ depends on both tensile and compressive concrete strength.

In most formulations, the fracture energy depends directly on the concrete tensile strength and on a shape factor that is function of the FRP-to-concrete width ratio (b_f / b_c). The formulations proposed by Neubauer and Rostasy (1997) and Lu et al. (2005), e.g., are:

$$G_f = 0.204 \cdot k_b^2 \cdot f_{ctm} \tag{2.41}$$

$$G_f = 0.308 \cdot \beta_w^2 \cdot \sqrt{f_{ctm}} \tag{2.42}$$

being f_{ctm} the mean tensile strength of concrete, k_b and β_w the shape factors defined as:

$$k_b = 1.06\sqrt{\frac{2 - b_f/b_c}{1 + b_f/400}}; \quad \beta_w = \sqrt{\frac{2 - b_f/b_c}{1 + b_f/b_c}} \tag{2.43}$$

Based on formulations of fracture energy similar to Eqs. (2.41) and (2.42) and on experimental results of bond tests, several theoretical formulations to evaluate the bond strength have been proposed in the past (Taljsten 1994; Neubauer and Rostasy 1997; Brosens and Van Gemert 1997; fib bulletin 2001; Chen and Teng 2001; Smith and Teng 2002; CNR-DT 200 2004). These expressions allow for predicting the end debonding load. In some cases, the same expressions are suitably modified by changing some factors in order to predict the intermediate crack debonding load in RC beams (Teng et al. 2003; Chen et al. 2006; CNR-DT 200 2004). The lay-out of these formulations is often similar, while the numerical coefficients calibrated on experimental results are different. Moreover, the safety factors, which are needed in order to calculate design provisions as part of the Limit State approach, are not always considered. This last point is an important issue, if a safety level (mean, characteristic or design) has to be associated to the provision.

The theoretical approaches suggested by fib bulletin 14 (2001), Chen and Teng (2001), CNR-DT 200 (2004) are considered. In particular, the bond strength expressed in terms of maximum tensile load in the FRP reinforcement, $N_{f,max}$, and the effective length, L_e, which is the minimum length required to full transfer the load, are defined as follows by the three approaches:

(1) fib bulletin 14 (2001):

$$N_{f,\max} = \alpha \cdot c_1 \cdot k_c \cdot k_b \cdot b_f \cdot \beta_L \cdot \sqrt{E_f \cdot t_f \cdot f_{ctm}}; \quad L_e = \sqrt{\frac{E_f \cdot t_f}{2 f_{ctm}}}$$
$$\beta_L = \frac{L_b}{L_e} \cdot \left(2 - \frac{L_b}{L_e}\right) \text{ if } L_b \le L_e, \quad \beta_L = 1 \text{ otherwise}; \ \frac{b_f}{b} \ge 0.33 \tag{2.44}$$

where b_f, t_f, E_f, L_b are width, thickness, Young's modulus and bonded length of the FRP reinforcement, b_c is the width of the concrete element, f_{ctm} is the mean tensile strength of concrete, $c_1 = 0.64$ and $c_2 = 2$ are coefficients related to an experimental calibration of the fracture energy (Neubauer and Rostasy 1997), $\alpha = 0.9$ is a reduction factor to account for the influence of inclined cracks on the bond strength, and k_c takes into account the state of compaction of concrete and usually is assumed equal to 1.00, or 0.67 for FRP bonded to concrete faces with low compaction. Finally, the shape factor k_b is given by Eq. (2.43).

(2) Chen and Teng (2001):

$$N_{f,\max} = \alpha \cdot \beta_w \cdot \beta_L \cdot b_f \cdot L_e \cdot \sqrt{f'_c}; \quad L_e = \sqrt{\frac{E_f \cdot t_f}{\sqrt{f'_c}}}$$
$$\beta_L = \sin\frac{\pi L_b}{2 L_e} \text{ if } L_b \le L_e, \quad \beta_L = 1 \text{ otherwise} \tag{2.45}$$

f'_c being the mean cylindrical compressive strength of concrete and α a coefficient equal to 0.427 or 0.315 to calculate a mean or a design provision, respectively. The shape factor β_w is given by Eq. (2.43). Note that the debonding strain values of Eq. (2.45) should be divided by an appropriate safety factor $\gamma_b = 1.25$ for design purpose, according to suggestion in Sect. 3.4 of Teng et al. (2001).

(3) CNR-DT 200 (2004):

$$N_{f,\max} = \frac{1}{\gamma_{f,d}\sqrt{\gamma_c}} \cdot \beta_L \cdot b_f \cdot \sqrt{k_G \cdot k_b} \cdot \sqrt{2 \cdot E_f \cdot t_f \cdot \sqrt{f_{ck} \cdot f_{ctm}}};$$
$$L_e = \sqrt{\frac{E_f \cdot t_f}{2 \cdot f_{ctm}}}$$
$$k_b = \sqrt{\frac{2 - b_f/b_c}{1 + b_f/400}} \ge 1 \ \beta_L = \frac{L_b}{L_e} \cdot \left(2 - \frac{L_b}{L_e}\right) \text{ if } L_b \le L_e, \ \beta_L = 1 \text{ otherwise} \tag{2.46}$$

where f_{ck} is the characteristic value of the cylindrical compressive strength of concrete and k_G is an experimentally calibrated coefficient, which is 0.064 or 0.03 for mean or design provision, respectively. The shape factor k_b is the same given by Eq. (2.43), except for the coefficient 1.06.

The safety factor for debonding failure, $\gamma_{f,d}$, is usually assumed equal to 1.2 or 1.5 (non-controlled or controlled gluing application), while γ_c is the safety factor for concrete (equal to 1.5).

Experimental Database

A lot of results have been collected from the technical literature concerning bond tests on concrete elements externally strengthened with CFRP cured in situ (sheets) and preformed (plates) systems. Several set-ups (Yao et al. 2005) have been realized by the researchers and each of them can be considered more or less reliable for the right prediction of the actual loading conditions and, thus, of the end debonding load in existing elements. Moreover, constructive detailing of specimens can influence the reliability of these results.

In this application, the only results of push-pull bond shear tests have been considered to perform the statistical analyses; moreover, the results of cured in situ and preformed systems have been distinguished in two different groups. In the push-pull test set-up (see Fig. 2.1) the concrete block is loaded by a pushing force that is applied at a certain distance, a, from the FRP reinforcement that is loaded in tension by a pulling action. Several experimental programs have shown that the push-pull set-up can be simply realized, according to different set-ups (Bilotta et al. 2009b). Such a set-up is less sensitive to construction details and, thus, furnishes low scattered results in terms of debonding loads. This is the reason for which it is widely used to predict the bond strength for both shear and flexural strengthening in RC beams (Yao et al. 2005).

The realization of bond tests where both the FRP reinforcement and the concrete block are loaded by tension forces (pull-pull scheme) requires special attention in detailing, especially concerning the symmetry of the reinforcements on the sides of the concrete specimens (Leone et al. 2009). In these schemes the set-ups are more sensitive to the geometrical inaccuracies and thus, the repeatability or the variability of the results can be strongly affected by detailing.

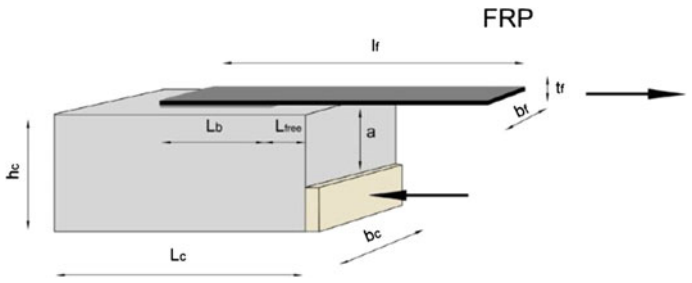

Fig. 2.1 General scheme of an asymmetrical push-pull bond test

In existing RC element (i.e. in RC beams) the FRP external reinforcement is usually applied on the tension side, so that the pull-pull scheme seems to replicate better the actual loading conditions. However, in the push-pull scheme, suitable values of the distance a (see Fig. 2.1) ensure the development of a bond failure at the concrete-FRP interface, similarly to what occurs in pull-pull scheme. On the contrary, for low values of a, the compressive stresses induced by the pushing force can limit the volume of concrete involved in the failure mechanism and, thus, furnish safe values of debonding load due to smaller values of fracture energy (see Eq. 2.40).

The results of specimens with bonded length, width and Young's modulus of the FRP reinforcement lower than 75 mm, 25 mm, and 80 GPa, respectively, were not considered.

For specimens strengthened with FRP sheets (Aiello and Leone 2005; Yao et al. 2005; Bilotta et al. 2009a; Ceroni and Pecce 2010; Lu et al. 2005; McSweeney and Lopez 2005; Takeo et al. 1997; Travassos et al. 2005; Ueda et al.1999; Wu et al. 2001; Zhao et al. 2000) the main parameters (see Fig. 2.1 for the geometrical parameters) vary in the following ranges: concrete width b_c = 100–500 mm, width of FRP reinforcement b_f = 25–100 mm, b_f/b_c = 0.17–1, thickness of FRP reinforcement t_f = 0.083–0.507 mm, bonded length of FRP reinforcement L_b = 75–500 mm, number of layers of FRP reinforcement n = 1–3, Young's modulus of FRP reinforcement E_f = 82–390 GPa, mean compressive strength of concrete f_{cm} = 17–62 MPa, and mean tensile strength of concrete f_{ctm} = 1.3–4.3 MPa.

Analogously, for specimens strengthened with FRP plates (Chajes et al. 1996; Faella et al. 2002; Mazzotti et al. 2009; Nigro et al. 2008; Bilotta et al. 2009a, b, 2011b) the main parameters vary in the following ranges: b_c = 150–230 mm, b_f = 25–100 mm, b_f/b_c = 0.11–0.63, t_f = 1.0–1.6 mm, n = 1, L_b = 150–400 mm, E_f = 108–400 GPa, f_{cm} = 15–53 MPa, and f_{ctm} = 1.10–3.8 MPa.

Totally, 216 data of bond tests for sheets and 68 for plates have been collected.

Calibration Procedure

According to the design assisted by testing approach, the random variable δ is defined as the ratio of the experimental debonding load, N_{exp}, to the theoretical one representing the strength model, N_{th}:

$$\delta_i = \frac{N_{\exp,i}}{N_{th,i}} \tag{2.47}$$

The mean value, the variance, the standard deviation and the CoV of this variable are defined as:

$$\overline{\delta} = \frac{1}{n}\sum_{i=1}^{n}\delta_i; \quad s_\delta^2 = \frac{1}{n-1}\sum_{i=1}^{n}(\delta_i - \delta)^2; \quad \sigma_\delta = \sqrt{s_\delta^2}; \quad CoV = \frac{\sigma_\delta}{\overline{\delta}} \tag{2.48}$$

The strength model expressed by N_{th} should be fine-tuned by a least-square coefficient, which minimizes the difference between each theoretical, $N_{th,i}$, and experimental, $N_{exp,i}$, value. Usually, this can be simply carried out considering the regression line of the graph $N_{th,i} - N_{exp,i}$. The slope of this line intercepting the origin furnishes the least-square coefficient, k_m.

Then, the random variable δ_m is defined as the ratio of the experimental debonding load N_{exp}, to the theoretical one, N_{th}, adjusted by means of the fine-tuning parameter, k_m:

$$\delta_{m,i} = \frac{N_{\exp,i}}{k_m \cdot N_{th,i}} \tag{2.49}$$

Mean value, variance, standard deviation and CoV of δ_m are defined as:

$$\begin{aligned} \overline{\delta_m} &= \frac{1}{n}\sum_{i=1}^{n}\delta_{m,i} = \frac{1}{n}\sum_{1=1}^{n}\frac{N_{\exp,i}}{k_m \cdot N_{th,i}} = \frac{\overline{\delta}}{k_m} \\ s_{\delta_m}^2 &= \frac{1}{n-1}\sum_{i=1}^{n}(\delta_{m,i} - \overline{\delta_m})^2 = \frac{1}{n-1}\sum_{i=1}^{n}\left(\frac{N_{\exp,i}}{k_m \cdot N_{th,i}} - \frac{\overline{\delta}}{k_m}\right) = \frac{s_\delta^2}{k_m} \end{aligned} \tag{2.50}$$

Thus, the mean provision for the debonding load can be assumed as:

$$N_{th,m} = k_m \cdot \overline{\delta_m} \cdot N_{th} \tag{2.51}$$

In Eq. (2.51) the model error is represented by the mean value of the variable δ_m, which is not 1, because the regression line was forced to intercept the origin.

In the Limit State approach, any strength is assumed as a random variable and, in general, the 0.05 percentile (named 'characteristic value') of its frequency distribution is used for design purposes. A very suitable distribution is the Gaussian one, but to use it the check of the normality hypothesis of the random variable is required. Several statistical tests (Shapiro-Wilk, Anderson-Darling, Martinez-Iglewicz, Kolmogorov-Smirnov, D'Agostino skewness, D'Agostino kurtosis, D'Agostino omnibus) can be performed (Mood et al. 1974; Shapiro and Wilk 1965) to verify the normality or log-normality hypothesis of the experimental distributions.

If the debonding load is assumed as a random variable and the Young's modulus of the FRP reinforcement, the tensile and compressive strength of concrete are assumed as the only parameters influencing the bond strength, the general expression of the strength model adjusted by the fine-tuning coefficient, k_m, is:

$$N_{th,m} = N_{th,m}\left(E_f, f_{cm}, f_{ctm}, \overline{\delta_m}, k_m\right) \tag{2.52}$$

Moreover, under the hypothesis of Gaussian distribution, the 0.05 percentile of the variable debonding load can be calculated as:

$$N_{th,k,0.05} = N_{th,m} - 1.64 \cdot \left[Var(N_{th,m})\right]^{0.5} \tag{2.53}$$

where the variance of $N_{th,m}$ can be expressed as:

$$\begin{aligned} Var\left(N_{th,m}\right) = {} & C_{Efm}^2 \cdot Var(Ef) + C_{fcm}^2 \cdot Var(fcm) + C_{fctm}^2 \cdot Var(fctm) \\ & + C_{\delta m}^2 \cdot Var(\delta_m) \end{aligned} \tag{2.54}$$

$$C_{Efm} = \left|\frac{\partial N_{th,m}}{\partial E_f}\right|_{\overline{E_f}}, \quad C_{f_{cm}} = \left|\frac{\partial N_{th,m}}{\partial f_{cm}}\right|_{\overline{f_{cm}}}, \quad C_{f_{ctm}} = \left|\frac{\partial N_{th,m}}{\partial f_{ctm}}\right|_{\overline{f_{ctm}}}, \quad C_{f_{ctm}} = \left|\frac{\partial N_{th,m}}{\partial \delta_m}\right|_{\overline{\delta_m}} \tag{2.55}$$

If Eqs. (2.54) and (2.55) are substituted in the Eq. (2.53), the 0.05 percentile of the debonding load becomes:

$$\begin{aligned} & N_{th,k,0.05} \\ & = N_{th,m} - 1.64 \cdot N_{th,m} \cdot \left[a \cdot CoV_{E_f}^2 + b \cdot CoV_{f_{cm}}^2 + c \cdot CoV_{f_{ctm}}^2 + CoV_{\delta_m}^2\right]^{0.5} \end{aligned} \tag{2.56}$$

where the coefficients a, b, c depend on the functional relation of N_{th} from the parameters E_f, f_{cm} and f_{ctm}. The $CoVs$ are defined for each parameter as the ratio of its mean value to the standard deviation:

$$CoV_{E_f} = \frac{\overline{E_f}}{s_{E_f}}, \quad CoV_{f_{ctm}} = \frac{\overline{f_{ctm}}}{s_{f_{ctm}}}, \quad CoV_{f_{cm}} = \frac{\overline{f_{cm}}}{s_{f_{cm}}}, \quad CoV_{\delta_m} = \frac{\overline{\delta_m}}{s_{\delta_m}} \tag{2.57}$$

Note that the standard deviations of E_f, f_{cm}, and f_{ctm} have been assessed according to some literature information:

$$s_{E_f} = 0.05 \cdot \overline{E_f}; \quad s_{f_{ctm}} = 0.183 \cdot \overline{f_{ctm}}; \quad s_{f_{cm}} = 4.88 \tag{2.58}$$

Clearly, the coefficient of variation of the variable δ_m, $\mathrm{CoV}_{\delta m}$, depends on the data distribution. Equation (2.56) can be written as:

$$N_{th,k,0.05} = k_k \cdot N_{th} \tag{2.59}$$

$$k_{k,0.05} = k_m \cdot \overline{\delta_m} \cdot \left(1 - 1.64 \cdot \left[a \cdot CoV_{E_f}^2 + b \cdot CoV_{f_{cm}}^2 + c \cdot CoV_{f_{ctm}}^2 + CoV_{\delta_m}^2\right]^{0.5}\right) \tag{2.60}$$

If the coefficients of variation of the materials are neglected, Eq. (2.60) becomes the well-known following one:

$$N_{th,k,0.05} = N_{th} \cdot \overline{\delta_m} \cdot k_m \cdot (1 - 1.64 \cdot CoV_{\delta_m}) = N_{th} \cdot k_m \cdot \left(\overline{\delta_m} - 1.64 \cdot s_{\delta_m}\right) \tag{2.61}$$

However, in this application all coefficients of variation have been taken into account. The percentiles 0.05 (characteristic values) are usually divided to safety factors, which take into account the model uncertainness (EN1990—Annex D). Furthermore, percentiles lower than 0.05 can be obtained by replacing in the Eq. (2.56) the coefficient 1.64 with the coefficients 2.58 and 3.08 corresponding to the 0.005 and 0.001 percentiles, respectively. These lower percentiles can be used as alternative to the characteristic values divided to the safety factors.

Application to the Experimental Database

The general Eq. (2.52) for debonding load can be particularized by introducing the dependence on the bond shear strength. Indeed, the bond shear strength depends on the concrete strength and can be related to the circle of Mohr representing the stress condition in the concrete at failure. Thus, different formulations for shear strength have been considered varying the dependence on the concrete strength. In particular, the following five expressions for the debonding load are examined:

$$\text{Case 1: } N_{th} = \beta_L \cdot b_f \cdot \sqrt{2 \cdot E_f \cdot t_f \cdot k_b \cdot \sqrt{f_{cm} \cdot f_{ctm}}} \tag{2.62}$$

$$\text{Case 2: } N_{th} = \beta_L \cdot b_f \cdot \sqrt{2 \cdot E_f \cdot t_f \cdot k_b \cdot f_{cm}^{2/3}} \tag{2.63}$$

$$\text{Case 3: } N_{th} = \beta_L \cdot b_f \cdot \sqrt{2 \cdot E_f \cdot t_f \cdot k_b \cdot f_{cm}^{0.6}} \tag{2.64}$$

$$\text{Case 4: } N_{th} = \beta_L \cdot b_f \cdot \sqrt{2 \cdot E_f \cdot t_f \cdot k_b \cdot \frac{f_{cm} \cdot f_{ctm}}{f_{cm} + f_{ctm}}} \tag{2.65}$$

$$\text{Case 5: } N_{th} = \beta_L \cdot b_f \cdot \sqrt{2 \cdot E_f \cdot t_f \cdot k_b \cdot 0.9 \cdot f_{ctm}} \tag{2.66}$$

In the Eq. (2.62), if a Coulomb failure criterion is adopted, the term $\sqrt{f_{cm} \cdot f_{ctm}}$ is 2 times the cohesion associated to the Mohr circle of an interface concrete element subjected to both shear and normal (peeling) stresses. The presence of peeling

stresses has been often experimentally evidenced by the visual inspection of the debonded surface configuration (Mazzotti et al. 2008). Thus, Case 1 reproduces better the actual physical phenomenon, because it takes into account both the presence of shear and normal interfacial stresses.

Moreover, in Eq. (2.63) the term $f_{cm}^{2/3}$ is a simplification of $\sqrt{f_{cm} \cdot f_{ctm}}$, if the concrete tensile strength is calculated by the Eq. (2.47).

Analogously in Eq. (2.65), the term $\frac{f_{cm} \cdot f_{ctm}}{f_{cm}+f_{ctm}}$ is the maximum shear stress compatible with the strength f_{cm} and f_{ctm} in an interface concrete element subjected to only shear stresses (the Mohr circle has centre in the axis origin in this case).

In Eq. (2.66), the term $0.9 \cdot f_{ctm}$ is a simplification of the term $\frac{f_{cm} \cdot f_{ctm}}{f_{cm}+f_{ctm}}$ under the assumption that the compressive strength is about 10 times the tensile one.

Finally in Eq. (2.64), the term $f_{cm}^{0.6}$ is a further modification of $0.9 \cdot f_{ctm}$ according to the expression for the concrete tensile strength given by Model Code 90.

$$f_{ctm} = 0.32 \cdot f_{cm}^{0.6} \tag{2.67}$$

For all cases the mean and the characteristic provisions of debonding load can be calculated using the previously introduced Eqs. (2.51) and (2.59):

$$N_{th,m} = k_m \cdot \overline{\delta_m} \cdot N_{th} \tag{2.68}$$

$$N_{th,k,0.05} = k_{k,0.05} \cdot N_{th} \tag{2.69}$$

where k_m is the least square coefficient associated to the regression line intercepting the origin, $\overline{\delta_m}$ is given by Eq. (2.16), and $k_{k,0.05}$ is given by Eq. (2.60).

For each equation, the best fitting coefficient k_m has been calculated considering the experimental results distinguished in two series: sheets and plates.

In Table 2.1 the coefficient k_m and the R^2 value of the corresponding least-square line, which is a measure of the reliability of the regression, are reported for all the

Table 2.1 Statistical data for different bond strength models

Case	FRP type	k_m	R^2	$\overline{\delta_m}$	CoV_{δ_m} (%)	$k_m \cdot \overline{\delta_m}$	$k_{k,0.05}$	$k_{k,0.005}$	$k_{k,0.001}$
1	Sheet	0.270	0.855	1.027	17.7	0.278	0.192	0.143	0.117
	Laminate	0.236	0.349	1.064	23.2	0.251	0.152	0.095	0.064
2	Sheet	0.258	0.878	1.010	17.6	0.261	0.182	0.137	0.112
	Laminate	0.221	0.534	1.034	20.4	0.229	0.149	0.103	0.078
3	Sheet	0.291	0.881	1.006	17.7	0.293	0.204	0.154	0.126
	Laminate	0.248	0.565	1.030	20.0	0.255	0.169	0.119	0.092
4	Sheet	0.535	0.862	1.022	17.6	0.547	0.370	0.269	0.214
	Laminate	0.466	0.375	1.060	23.0	0.496	0.294	0.180	0.118
5	Sheet	0.544	0.863	1.021	17.5	0.555	0.375	0.270	0.213
	Laminate	0.473	0.379	1.059	22.9	0.502	0.297	0.180	0.117

equations. The mean value of the variable δ_m, defined by Eqs. (2.50) and (2.51), and its CoV are reported too. In all cases the CoV, which is a measure of the model significance, is lower than the threshold value of 40 % (Monti et al. 2009), so that all the models can be considered reliable. However, it can be observed that, while for the sheets the R^2 value is low sensitive to the model and is quite elevated (0.855–0.881), on the contrary for the plates the choice of the model can be significant considering that R^2 varies in the range 0.349–0.565. Despite their better quality control in factory, the preformed FRP systems present a higher CoV and a smaller R^2 value with respect to the in situ sheets. This is justifiable by the larger sensitivity of this system to the detailing of the experimental procedure. Indeed, increasing the stiffness of the FRP system results in more inaccuracies of the experimental set-up, which can influence the debonding load.

In particular, Case 3 results the best-fitting model because of the highest value of R^2; this relationship depends on the compressive strength of concrete with an exponent 0.6. Note that for design aim, the choice of the best-fitting model has the clear advantage to furnish characteristic values more close to the mean ones, because the theoretical loads show a smaller gap with the experimental results.

In Table 2.1 the coefficients k_k to calculate different percentiles (5, 0.5, and 0.1 %) are reported too. The coefficients $k_m \cdot \overline{\delta_m}$, which allow for calculating the mean provisions, differ of about 12–15 % for the sheets and the plates. The factors $k_{k,0.05}$, which allow for calculating the 0.05 percentiles, differ of about 17–21 %.

The general Eq. (2.52) for the mean provision for the best-fitting model (Case 3) is:

$$N_{th,m} = k_m \cdot \delta_m \cdot \beta_L \cdot b_f \cdot \sqrt{2 \cdot E_f \cdot t_f \cdot k_b \cdot f_{cm}^{0.6}} \tag{2.70}$$

The corresponding 0.05 percentile provision given by Eqs. (2.56) and (2.60) is:

$$\begin{aligned} N_{th,k,0.05} &= N_{th,m} - 1.64 \cdot N_{th,m} \cdot \left[0.5^2 \cdot CoV_{E_f}^2 + (3/10)^2 \cdot CoV_{f_{cm}}^2 + CoV_{\delta_m}^2\right]^{0.5} \\ &= k_k \cdot N_{th} \end{aligned} \tag{2.71}$$

$$k_{k,0.05} = k_m \cdot \delta_m \cdot \left[1 - 1.64 \cdot \left[0.5^2 \cdot CoV_{E_f}^2 + (3/10)^2 \cdot CoV_{f_{cm}}^2 + CoV_{\delta_m}^2\right]^{0.5}\right] \tag{2.72}$$

$$\begin{aligned} C_{Efm} &= \left|\frac{\partial N_{th,m}}{\partial E_f}\right|_{\overline{E_f}} = N_{th,m} \cdot \frac{0.5}{\overline{E_f}}, \\ C_{Efm}^2 \cdot Var(Ef) &= N_{th,m}^2 \cdot \frac{0.5^2}{\overline{E_f^2}} \cdot Var(E_f) = N_{th,m}^2 \cdot 0.5^2 \cdot CoV_{E_f}^2 \end{aligned} \tag{2.73}$$

$$C_{f_{cm}} = \left|\frac{\partial N_{th,m}}{\partial f_{cm}}\right|_{\overline{f_{cm}}} = N_{th,m} \cdot \frac{3/10}{\overline{f_{cm}}},$$
$$C_{fcm}^2 \cdot Var(f_{cm}) = N_{th,m}^2 \cdot \frac{(3/10)^2}{\overline{f_{cm}^2}} \cdot Var(f_{cm}) = N_{th,m}^2 \cdot (3/10)^2 \cdot CoV_{f_{cm}}^2 \tag{2.74}$$

$$C_{f_{ctm}} = \left|\frac{\partial N_{th,m}}{\partial \delta_m}\right|_{\overline{\delta_m}} = \frac{N_{th,m}}{\overline{\delta_m}},$$
$$C_{\delta m}^2 \cdot Var(\delta_m) = N_{th,m}^2 \cdot \frac{Var(\delta_m)}{\overline{\delta_m}} =, \quad N_{th,m}^2 \cdot CoV^2 \delta_m \tag{2.75}$$

$$C_{f_{ctm}} = \left|\frac{\partial N_{th,m}}{\partial f_{ctm}}\right|_{\overline{f_{ctm}}} = 0 \tag{2.76}$$

The last term related to the tensile strength of concrete, f_{ctm}, is clearly absent, because the debonding load in Eq. (2.64) depends only on the compressive strength.

However, as it occurs for all other cases, the variance of the materials is less significant compared with the variance of the model. Indeed, for the cured in situ systems the coefficient of variation of the variable δ_m is:

$$CoV_{\delta_m} = \frac{\overline{\delta_m}}{s_{\delta_m}} = \frac{1.006}{0.178} = 0.177 \rightarrow CoV_{\delta_m}^2 = 0.031 \tag{2.77}$$

By contrast, the contributes related to the CoVs of the materials are:

$$0.5^2 \cdot CoV_{E_f}^2 + (3/10)^2 \cdot CoV_{f_{cm}}^2 = 0.0026 \approx 0.003 \approx 0.1 \cdot CoV_{\delta_m}^2$$

In Fig. 2.2 the experimental debonding loads are compared with the theoretical ones given by Case 3—Eq. (2.64); the regression line intercepting the origin of axis is reported too. Figure 2.2a refers to the cured in situ systems and Fig. 2.2b to the preformed ones.

In Fig. 2.3 the experimental values of strain in the FRP reinforcement at debonding are plotted together with the mean and characteristic provisions given by Eq. (2.64) using the values of k_m and k_k, for the three percentiles 5, 0.5, and 0.1 %, listed in Table 2.1. The characteristic provision (5 % percentile) divided to the safety factor $\gamma_f = 1.2$ (related to good application conditions, according to CNR-DT 200 2004) is plotted too.

Both theoretical and experimental strains are plotted vs. the term $E_f \cdot t_f / 2 \cdot \Gamma_f$, assuming $\Gamma_f = k_b \cdot f_{cm}^{0.6}$ according to Eq. (2.64). This allows for graphing the theoretical curves normalized to the axial stiffness of the FRP reinforcement and the concrete strength.

The theoretical curves show that the 0.5 % percentile can be a good choice to warrant a reliable safety level to the aim of furnish design provisions. Note that the

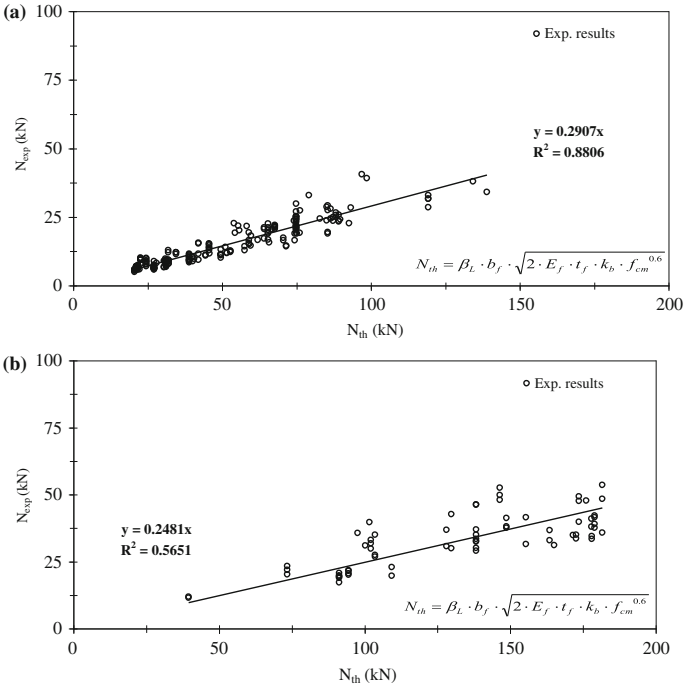

Fig. 2.2 Regression line: **a** cured in situ systems: 216 data; **b** preformed systems: 68 data

assessment of the percentiles has been carried out taking into account the variance of the materials.

Another possibility, which is adopted by the Italian guidelines (CNR–DT 200 2004) and, more in general, is included in the Eurocode approach, consists into divide the characteristic provision (5 % percentile) to a safety factor γ_f that depends on the quality of the application. Figure 2.3 shows that the provisions corresponding to the 5 % percentile divided to the factor $\gamma_f = 1.2$ are, however, less safe than the 0.5 % percentile.

It should be noted that the percentiles provisions were calculated under the hypothesis of Gaussian distribution. Some statistical tests (Shapiro-Wilk, Anderson-Darling, Martinez-Iglewicz, Kolmogorov-Smirnov, D'Agostino skewness, D'Agostino kurtosis, D'Agostino omnibus) were performed to verify this assumption but the comparison between the cumulate frequency curves of N_{exp} and the Gaussian distribution, having the same mean value and standard deviation, highlighted a bad agreement, especially for the cured in situ sheets. This was confirmed also by the responses of the statistical tests, which in most cases rejected the normality assumption for sheets and accepted it for plates. For the sheets, the experimental debonding loads seemed better represented by a log-normal distribution.

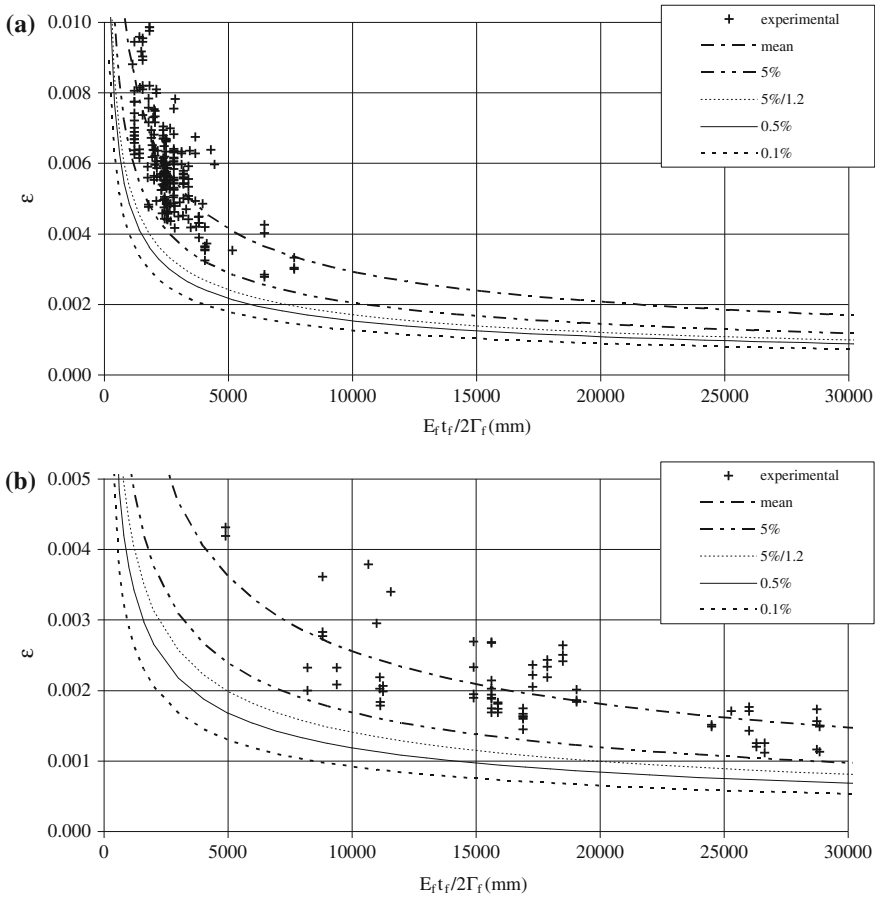

Fig. 2.3 Experimental versus theoretical failure strains: **a** cured in situ systems (216 data); **b** preformed systems (68 data)

However, the values of percentiles calculated under the hypothesis of log-normal distributions are larger than the ones reported in Table 2.1 (Gaussian distribution). Thus, the normal distribution can be considered safe to the aim of furnishing design provisions.

Finally, in Tables 2.2 and 2.3 the mean value, the standard deviation, and the CoV of the ratio N_{th}/N_{exp} are reported for both cured in situ (sheets) and preformed systems (plates).

The theoretical values N_{th} given by the new proposal refer to both mean (Eq. 2.34) and characteristic provisions (Eq. 2.35); in particular the percentiles 0.05 and 0.005 have been considered. The characteristic provision (5 % percentile) divided to $\gamma_f = 1.2$ is reported too. Finally, the design provisions of CNR-DT 200 (2004), Teng et al. (2001) are also listed. The characteristic provisions were divided

Table 2.2 Values of the ratio N_{th}/N_{exp} for cured in situ FRP systems (216 results)

N_{th}/N_{exp}	New calibration				Design	
	$N_{th,m}$	$N_{th,k,0.05}$	$N_{th,k,0.05}/1.2$	$Nt_{h,k,0.005}$	CNR DT 200 (2004)	Teng et al. (2001)
Mean	1.03	0.72	0.60	0.54	0.43	0.54
St. dev.	0.173	0.121	0.101	0.091	0.083	0.08
CoV (%)	16.8	16.8	16.8	16.8	19.4	15.7

Table 2.3 Values of the ratio N_{th}/N_{exp} for preformed FRP systems (68 results)

N_{th}/N_{exp}	New calibration				Design	
	$N_{th,m}$	$N_{th,k,0.05}$	$N_{th,k,0.05}/1.2$	$N_{th,k,0.005}$	CNR DT 200 (2004)	Teng et al. (2001)
Mean	1.03	0.68	0.57	0.48	0.47	0.63
St. dev.	0.20	0.13	0.11	0.09	0.12	0.120
CoV (%)	19.1	19.1	19.1	19.1	25.1	19.1

to the safety factors: $\gamma_f = 1.2$ and $\sqrt{\gamma_c} = \sqrt{1.5}$ for CNR-DT 200 2004; $\gamma_b = 1.25$ for Teng et al. 2001.

The results of Tables 2.2 and 2.3 show that the mean ratio $N_{th,m}/N_{exp}$ is approximately 1 for both systems. The mean value of $N_{th,k,0.05}/N_{exp}$ for the sheets is slightly larger than the ones given by Eqs. (2.46) and (2.45): 0.72 versus 0.63 and 0.67 respectively (see Table 2.1).

By contrast, for plates, the mean value of $N_{th,0.05}/N_{exp}$ is slightly lower than the one given by Eq. (2.46) (0.68 vs. 0.70, see Table 2.1) and sensibly lower than the one given by Eq. (2.45) (0.68 vs. 0.79, see Table 2.1). However, these differences relate to mean values of the ratio N_{th}/N_{exp} and, thus, can be misleading to compare the predictions of different models. In contrast, the curves of Fig. 2.4, where experimental and theoretical debonding strains of the only FRP sheets are plotted

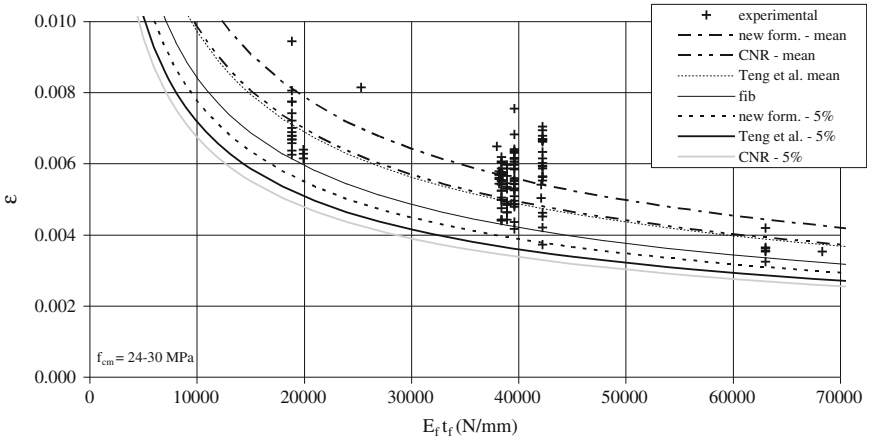

Fig. 2.4 Experimental maximum strain versus mean and 0.05 percentile provisions for sheets

vs. the parameter $E_f \cdot t_f$, show the actual variations between the different formulations examined. Since the theoretical strain depends on the concrete strength, a range of variability for this parameter has been fixed (24–30 MPa that corresponds to a mean value of about 27 MPa). The mean and characteristic (5 % percentile) provisions ($N_{th,k,0.05}$) given by the new formulation, by (CNR-DT 200 2004) and by (Chen and Teng 2001) are plotted in the graph. In particular, both mean and characteristic provisions (5 % percentile) given by the new formulation are larger than the predictions of (Chen and Teng 2001) and (CNR-DT 200 2004). Moreover, the formulation of (CNR-DT-200 2004) gives the most safe results in terms of 5 % percentile, while furnishes mean predictions very similar to (Chen and Teng 2001). Furthermore, it can be observed that the formulation of (fib bulletin 14 2001), lies between the mean and the characteristic curves given by the new formulation.

In Fig. 2.5 several design proposals coming from the new formulation (0.01, 0.5, and 5 % percentile divided to $\gamma_f = 1.2$), the model of fib bulletin 14 (2001), the design provisions of CNR-DT 200 (2004) and Teng et al. (2001) are plotted together with the experimental debonding strains of the same tests considered in Fig. 2.4.

For the sheets, the graph of Fig. 2.5a shows that two design proposals coming from the new formulation (5 % percentile divided to 1.2 and 0.5 % percentile) are less safe than the ones currently furnished by CNR-DT 200 (2004). Note that the latter introduces the additionally safety factor of concrete, $\sqrt{\gamma_c}$, for design. This coefficient has been omitted in the new formulation because the variance of the concrete has been taken into account in the calibration procedure by means of the CoV of its compressive strength (see Eq. 2.72). Moreover, it can be observed that, the current design values of CNR-DT 200 (2004) are comparable with the 0.1 % percentile provisions of the new formulation. By contrast, the design formulation of Teng et al. (2001) is comparable with the 0.5 % percentile of the new formulation. Finally for the cured in situ systems, if the 0.5 % percentile of the new formulation is chosen as design provision, the debonding load increases of about +25 % compared with the current CNR provisions and is comparable with the design values of Teng et al. (2001).

On the contrary, in case of plates, Fig. 2.5b shows that the 0.5 % percentile of the new formulation is comparable with those currently furnished by CNR-DT 200 (2004), while the 5 % percentile divided to 1.2 is less safe (about 15 %). Moreover, the design formulation of Teng et al. (2001) is less safe compared with both the 5 % percentile of the new formulation divided to 1.2 and the 0.5 % one.

In conclusion, the proposed formulation for the end debonding load has a clear statistical meaning and allows for separating the provisions for the cured in situ FRP systems and the preformed ones. This distinction is mainly due to the larger scatter of the experimental results collected for this strengthening system.

Both aspects let to better exploit the strength of the cured in situ systems; indeed the 0.05 % percentile values of the new formulation are larger than the design values furnished by the current Italian Guidelines and, however, allow for assessing the same safety level of model of Teng et al. (2001). Moreover, it is worth noticing that the formulation of fib Bulletin 14 (2001) results excessively unsafe compared to the experimental results.

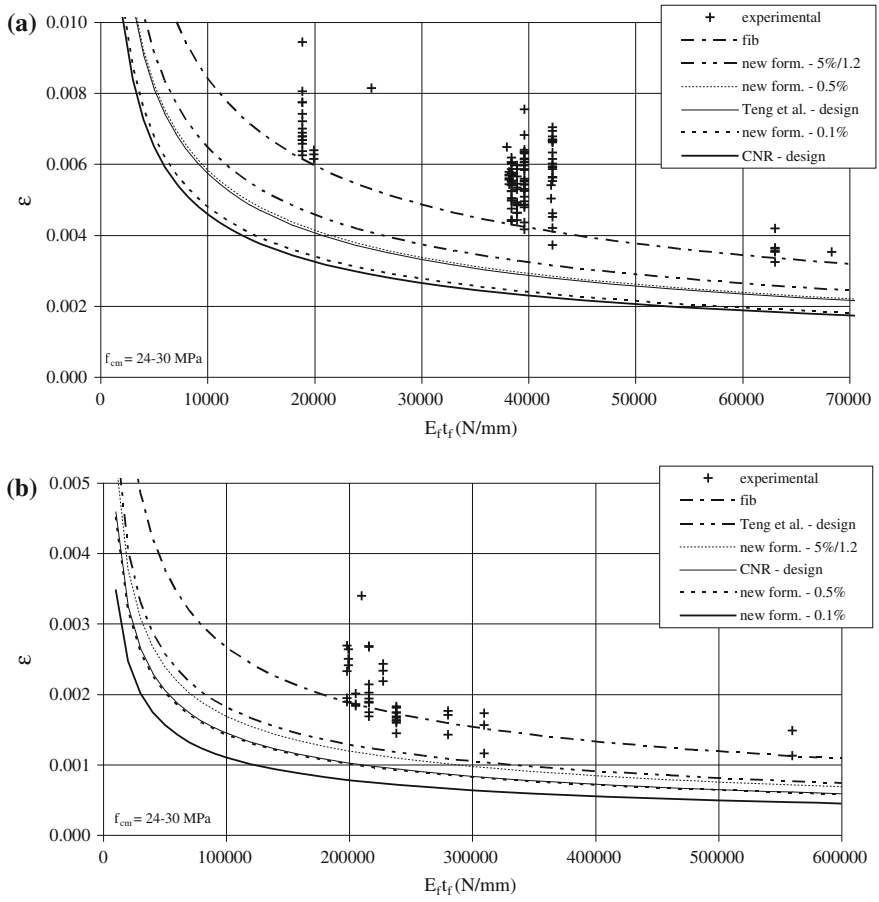

Fig. 2.5 Experimental maximum strain versus design provisions: **a** sheets; **b** plates

By contrast, the approach of Teng et al. (2001) and fib Bulletin 14 (2001) are found to be less safe when applied to preformed systems. Moreover, the 0.5 % percentile of the proposed design formulation provides a higher safety level compared with these models, while is similar to the current design provisions of CNR-DT 200 (2004). Thus, these results confirm that the distinction of the two strengthening systems seem to be reliable in predicting the debonding load.

Application 2—Intermediate Debonding

In this section the procedure is used to calibrate a design relationship for intermediate debonding on a wide database assembled by collecting data of experimental tests on FRP-strengthened RC beams.

Experimental Database

The database was obtained by merging the data considered by Ferracuti et al. (2007) with those collected by Wu and Niu (2007) and about thirty further experimental cases reported in the scientific literature (Beber 1999, 2003; Grace et al. 1999; Khomwan et al. 2004; Pham and Al-Mahaidi 2004; Sharif et al. 1991; Triantafillou and Plevris 1992). The resulting database collects the geometric and mechanical data describing the RC beams and their steel and composite reinforcement, the latter being made of externally bonded composite laminates based on carbon, glass or aramid fibers.

For specimens strengthened with FRP systems cured in situ (sheets), the relevant geometric and mechanical parameters range in the following intervals: concrete width b_c = 75–960 mm, FRP width b_f = 30–480 mm, b_f/b_c = 0.17–1, FRP thickness t_f = 0.11–2.55 mm, Young's modulus of FRP E_f = 21–390 GPa, mean compressive strength of concrete f_{cm} = 21–61 MPa, mean tensile strength of concrete f_{ctm} = 2.3–4.3 MPa.

For specimens strengthened with preformed FRP systems (laminates), the key parameters vary in the following ranges: concrete width b_c = 180–800 mm, FRP width b_f = 25–280 mm, b_f/b_c = 0.13–1, FRP thickness t_f = 1.0–6 mm, Young's modulus of FRP E_f = 190–220 GPa, mean compressive strength of concrete, f_{cm} = 12.6–53.4 MPa, mean tensile strength of concrete, f_{ctm} = 1.62–4.25 MPa.

A total number of 214 experimental results have been collected (164 FRP cured in situ systems and 50 FRP preformed system).

Intermediate debonding failure have been observed in all these tests. In principle, the maximum bending moment M_{db} observed in the experimental tests at debonding is smaller than the ultimate one M_u, corresponding to FRP rupture. The following parameter γ could be introduced for quantifying how premature is failure with respect to the ultimate flexural strength:

$$\gamma = \frac{M_{db} - M_y}{M_u - M_y} \tag{2.78}$$

M_y being the bending moment of the strengthened section at yielding of rebar: both M_u and M_y can be determined theoretically adopting the usual assumptions for RC sections at ULS. The parameter γ is closer to zero as debonding occurs for small values of the maximum axial strain in FRP; on the contrary, it is close to the unity as axial strain at debonding is close to the corresponding ultimate value $\varepsilon_{f,u}$. Figure 2.6 points out that the values of γ determined for the beams collected in the database generally range between zero and one; only in few cases (less than ten out of the total 214) it is slightly larger than the unity, mainly as a result of hardening of the materials.

The values of γ have been represented in Fig. 2.6 against the square root of the ratio between (twice) the fracture energy, G_F, and the specific axial stiffness of the FRP reinforcement, $E_f t_f$; the former parameter has been evaluated as a function of

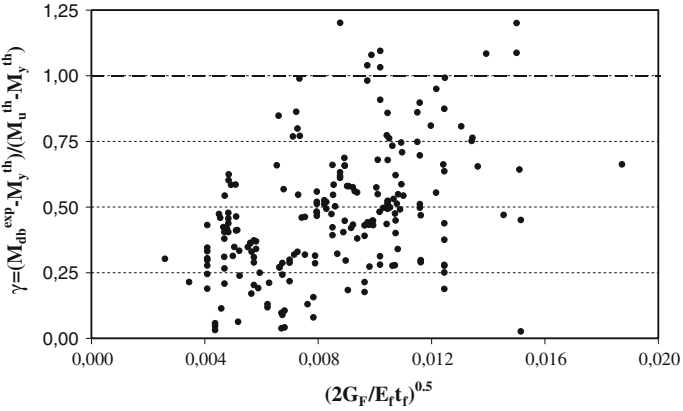

Fig. 2.6 Values of γ parameter against some mechanical parameters

both concrete tensile, f_{ct}, and compressive, f_c, strengths through the relation proposed in the Italian Code. The ratio $2G_F/E_f t_f$ is often considered in various proposals as the key parameter for determining the value of axial strain ε_{db} developed in FRP at debonding onset. However, Fig. 2.6 can only point out a general trend resulting in values of γ as large as the parameter represented on the x-axis, but it is quite hard to recognize a consistent correlation between γ (or, even, the maximum axial strain ε_{db} developed in FRP at debonding) and the quantity on the x-axis possibly depending on the two following reasons:

- fracture energy, G_F, basically depends on concrete (tensile) strength and, consequently, is widely scattered;
- besides the one reported on the x-axis, other parameters play an important role on the occurrence and extent of debonding failure.

For instance, the role of both the amount of steel rebar and their yielding stress/strain values have been emphasized in Faella et al. (2008a). Furthermore, load distribution also affects the possible premature failure of FRP strengthened beams as confirmed by Fig. 2.7 showing a strict correlation between the yielding moment M_y of the strengthened section and the maximum bending moment at debonding M_{db} at least in the case of three- or four-point-bending, while a completely different behavior results in the case of uniformly distributed load.

Figure 2.8 shows the distribution of the parameter γ for the experimental results considered within the database. It points out that such values are quite uniformly distributed since the cumulative frequency distribution is not so far from the ideally uniform straight curve, meaning that cases of very premature debonding are considered within the database as well as other cases whose failure is close to the complete development of the strength on the external reinforcement.

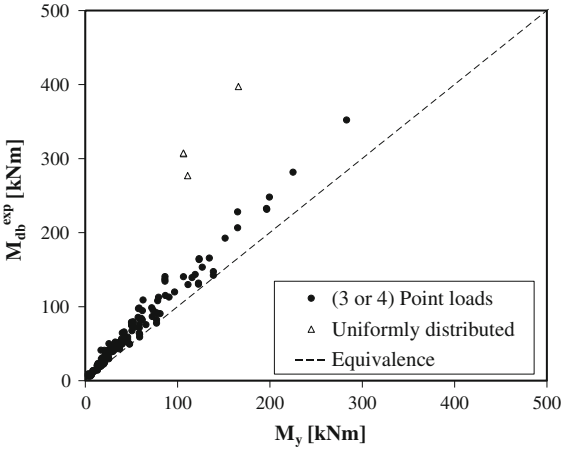

Fig. 2.7 Relation between bending moment at debonding and yielding

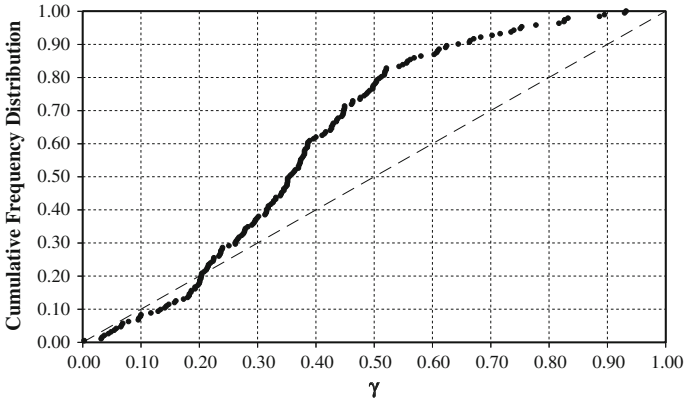

Fig. 2.8 Distribution of the parameter γ within the experimental database

Finally, it is worth noting that only the experimental results characterized by values of $\gamma \in (0,1)$ will be considered in the following, as that is a necessary condition for recognizing the cases of beams failure in intermediate debonding.

Procedure and Application

As already shown in the previous section for the end debonding, the mean value of the maximum axial strain in FRP corresponding to failure in intermediate crack-induced debonding (IC debonding strain) can be expressed by means of a

relationship obtained by a deterministic model and fine-tuned on experimental data by a numerical coefficient k_{IC}. The assessment of k_{IC} through the design by testing procedure gives a clear probabilistic meaning to the provisions.

An error function δ can cover the uncertainties of the simplified model considered in the above mentioned calibration:

$$\varepsilon_{fd} = \varepsilon_{fd,m}\left(k_{IC}, f_c, f_{ct}, E_f, t_f, b_f, k_b\right) \cdot \delta \tag{2.79}$$

The random variable δ is defined, for each ith test, as the ratio of the experimental debonding strain, $\varepsilon_{exp,i}$, to the theoretical one, $\varepsilon_{fd,m}$ evaluated by considering the geometric and mechanical data characterizing that test:

$$\delta_i = \frac{\varepsilon_{\exp,i}}{\varepsilon_{th,i}} \tag{2.80}$$

Moreover, the mean value, the variance, the standard deviation and the CoV of this variable are defined as:

$$\overline{\delta} = \frac{1}{n}\sum_{i=1}^{n}\delta_i; \quad s_\delta^2 = \frac{1}{n-1}\sum_{i=1}^{n}(\delta_i - \overline{\delta})^2; \quad \sigma_\delta = \sqrt{s_\delta^2}; \quad CoV = \frac{\sigma_\delta}{\overline{\delta}} \tag{2.81}$$

By assuming a formulation similar to design Eq. (2.60), taking into account no safety partial factors the relationship (2.79) can be rewritten as follows:

$$\varepsilon_{fd,m}\left(k_{IC}, f_c, f_{ct}, E_f, t_f, b_f, k_b\right) = k_{IC} \cdot \sqrt{\frac{2 \cdot k_b \cdot \sqrt{f_c \cdot f_{ct}}}{E_f t_f}} \tag{2.82}$$

The coefficient k_{IC} has been calibrated based on experimental results in terms of deformation $\varepsilon_{fd,exp}$ obtained by using the procedure in Faella et al. (2010) as stated above. The calibration has achieved using a least-square procedure consisting in the resolution of the following minimum problem:

$$k_{IC,m} = \arg\min_{k_{IC}} \sum_{i=1}^{n}\left[\varepsilon_{fd,m}\left(k_{IC}, f^{(i)}, f_{ct}^{(i)}, E_f^{(i)}, t_f^{(i)}, b_f^{(i)}, k_b^{(i)}\right) - \varepsilon_{fd,\exp}^{(i)}\right]^2 \tag{2.83}$$

Moreover, the mean value of the intermediate debonding strain can be obtained by a coefficient $k_{IC,m}$ adjusted by means of the mean value of the error parameter $\overline{\delta}$, being in general $\overline{\delta} \neq 1$ because the regression line was imposed to intercept the origin.

$$k_{IC,m} = k_{IC,bf} \cdot \overline{\delta} \tag{2.84}$$

Thus, the mean provision for the intermediate debonding strain can be assumed as:

$$\varepsilon_{th,m} = k_{IC,m} \cdot \varepsilon_{th} \tag{2.85}$$

being ε_{th} the strain obtained by the deterministic model. Obviously, this strain is linearly proportional to the debonding strain being the FRP constitutive law linear elastic.

If the random variable represents strength, its characteristic value is often defined for design purposes as the 0.05 percentile of the frequency distribution associated to the examined variable. Gauss distribution is the most generally considered for describing the errors. The so-called "hypothesis of normal distribution" for the variable δ should be checked by comparing the experimental curve of the cumulative frequency to the theoretical one corresponding to a Gaussian distribution having the same mean value and standard deviation (see Fig. 2.9).

Assuming that the Young's modulus, E_f, of the FRP reinforcement, the concrete tensile and compressive strength, f_{ctm} and f_c, are the only mechanical parameters influencing the value of the maximum axial strain developed in FRP at debonding, the expressions for the general and calibrated models involving the coefficient $k_{IC,bf}$ as well as $\overline{\delta}$ are:

$$\varepsilon_{th} = \varepsilon_{th}\left(E_f, f_{cm} f_{ctm}\right) \tag{2.86}$$

$$\varepsilon_{th,m} = \varepsilon_{th,m}\left(E_f, f_{cm} f_{ctm}, \overline{\delta}, k_{IC,bf}\right) \tag{2.87}$$

In the following, the same assumptions already considered above in defining a characteristic value for plate end debonding strength are accepted (Bilotta et al. 2011). In particular, both E_f and f_c and f_{ct} have been assumed as normally and independently distributed random variables, with the following values of the coefficients of variation:

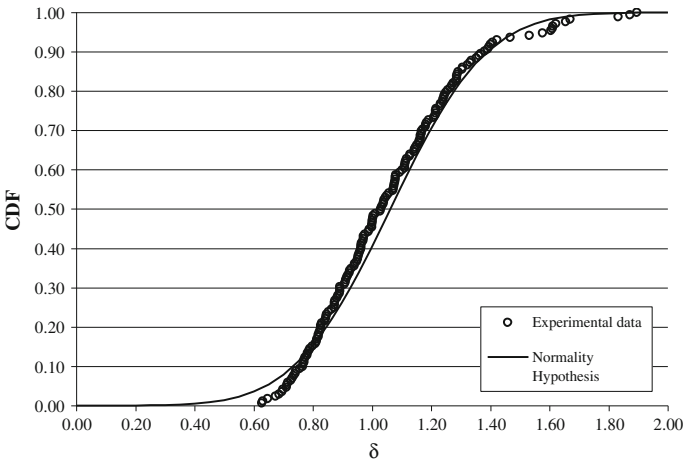

Fig. 2.9 Experimental data cumulative frequency against theoretical in normality hypothesis

$$s_{E_f} = 0.05 \cdot \overline{E_f} \quad s_{f_{ctm}} = 0.183 \cdot \overline{f_{ctm}} \quad s_{f_{cm}} = 4.88, \tag{2.88}$$

according to the design relationships provided by EN 1992-1-1 and literature information (Di Ludovico et al. 2009).

Hence, under the hypothesis of normal distribution for the variable δ, the provision corresponding to the 0.05 percentile of the Gaussian distribution is:

$$\varepsilon_{th,k} = \varepsilon_{th,m} - 1.64 \cdot \left[Var(\varepsilon_{th,m})\right]^{0.5} \tag{2.89}$$

where the variance of $\varepsilon_{th,m}$ can be expressed as:

$$\begin{aligned} Var\left(\varepsilon_{th,m}\right) = {} & C_{Efm}^2 \cdot Var(Ef) + C_{fcm}^2 \cdot Var(fcm) \\ & + C_{fctm}^2 \cdot Var(fctm) + C_{\delta m}^2 \cdot Var(\delta_m) \end{aligned} \tag{2.90}$$

$$\begin{aligned} C_{Efm} &= \left|\frac{\partial \varepsilon_{th,m}}{\partial E_f}\right|_{\overline{E_f}} \\ C_{f_{cm}} &= \left|\frac{\partial \varepsilon_{th,m}}{\partial f_{cm}}\right|_{\overline{f_{cm}}} \\ C_{f_{ctm}} &= \left|\frac{\partial \varepsilon_{th,m}}{\partial f_{ctm}}\right|_{\overline{f_{ctm}}} \\ C_{f_{ctm}} &= \left|\frac{\partial \varepsilon_{th,m}}{\partial \delta_m}\right|_{\overline{\delta_m}} \end{aligned} \tag{2.91}$$

If Eqs. (2.90) and (2.91) are substituted in Eq. (2.89), the following general expression is obtained for the characteristic provision of the debonding load:

$$\varepsilon_{th,k} = \varepsilon_{th,m} - 1.64 \cdot \varepsilon_{th,m} \cdot \left[a \cdot CoV_{E_f}^2 + b \cdot CoV_{f_{cm}}^2 + c \cdot CoV_{f_{ctm}}^2 + CoV_{\delta_m}^2\right]^{0.5} \tag{2.92}$$

where the coefficient a, b, c depend on the functional relationship of E_f, f_{cm} and f_{ctm} in the expression of ε_{th} and the coefficients of variation are defined for each parameter as the ratio of the mean value to its standard deviation:

$$CoV_{E_f} = \frac{\overline{E_f}}{s_{E_f}}, \quad CoV_{f_{ctm}} = \frac{\overline{f_{ctm}}}{s_{f_{ctm}}}, \quad CoV_{f_{cm}} = \frac{\overline{f_{cm}}}{s_{f_{cm}}} \quad CoV_{\delta_m} = \frac{\overline{\delta_m}}{s_{\delta_m}}, \tag{2.93}$$

Clearly the coefficient of variation of the variable δ_m, $CoV_{\delta m}$, depends on the data distribution. Equation (2.92) can be written as:

$$\varepsilon_{th,k} = k_{cr,k} \cdot \varepsilon_{th} \tag{2.94}$$

assuming:

$$k_{cr,k} = k_{cr,m} \cdot \left(1 - 1.64 \cdot \left[a \cdot CoV_{E_f}^2 + b \cdot CoV_{f_{cm}}^2 + c \cdot CoV_{f_{ctm}}^2 + CoV_{\delta_m}^2\right]^{0.5}\right) \tag{2.95}$$

As already stated in the application related to the end-debonding phenomenon, lower percentiles can be obtained by substituting in Eq. (2.95) the coefficient 1.64, related to the 0.05 percentile of the frequency distribution, with the coefficients 2.58 and 3.08 corresponding to the 0.005 and 0.001 percentiles, respectively.

The use of percentiles lower than 0.05 can be alternative to the use of safety factors that usually have to be additionally applied to characteristic provision to take into account the model uncertainness (EN1990—Annex D).

The following values of the coefficients defined above have been derived by considering the experimental results in a least-square procedure:

$$k_{IC,bf} = 0.53, \quad k_{IC,,m} = 0.56, \quad k_{IC,5\%} = 0.32 \text{ and } k_{IC,0.5\%} = 0.18. \tag{2.96}$$

From the coefficients $k_{IC,m}$ and $k_{IC,5\%}$ the following coefficients can be easily defined:

$$\begin{aligned} k_{Gm,2} &= \left(k_{IC,m}\right)^2 = 0.32\,\text{mm} \\ k_{Gk,2} &= \left(k_{IC,k}\right)^2 = 0.10\,\text{mm} \end{aligned} \tag{2.97}$$

These coefficients provide a clear statistical meaning to the formulation proposed to assess the intermediate debonding strain.

References

ACI Committee 318. (2005). Building Code Requirements for Structural Concrete (ACI 318–05) and Commentary (318R-05) (p. 430). Farmington Hills: American Concrete Institute.

ACI Committee 440.2 R-08. (2008). Guide for the Design and Construction of Externally Bonded FRP Systems for Strengthening Concrete Structures.

Aiello, M. A., & Leone, M. (2005). Experimental bond analysis of concrete-FRP (fiber reinforced polymer) reinforced. *Proceedings of fib Symposium* "*Keep Concrete Attractive*", *Budapest*, *Hungary*.

Ang, A. H. S., & Tang, W. H. (1975). Probability concepts in engineering planning and decision. Basic principles (Vol. 1). New York: Wiley.

Arduini, M., & Nanni, A. (1997). Behavior of precracked RC beams strengthened with carbon FRP Sheets. *Journal of Composites for Construction, 1*(2), 63–70.

Beber, A. J. (2003). *Comportamento Estrutural de Vigas de Concreto Armado Reforçadas com Compósitos de Fibra de Carbono*. UFRGS, Porto Alegre: Tese de Doutorado. (in Portuguese).

Bilotta, A., Ceroni, F., Di Ludovico, M., Nigro, E., & Pecce ,M. (2011a). Bond tests on concrete elements strengthened with EBR and NSM FRP systems, *Proceedings Of FRP RCS 10*, April 2–4, 2011, Tampa, Florida, USA.

Bilotta, A., Ceroni, F., Di Ludovico, M., Nigro, E., & Pecce, M. (2011b). Design by testing of debonding load in RC element strengthened with EBR FRP materials, *Proceedings Of FRP RCS 10*, April 2–4, 2011, Tampa, Florida, USA.

Bilotta, A., Ceroni, F., Di Ludovico, M., Nigro, E., Pecce, M., & Manfredi, G. (2011). Bond efficiency of EBR and NSM FRP systems for strengthening concrete members, *Journal of Composites for Construction*, (Vol. 15, Issue 5, pp 757–772), DOI: 10.1061/(ASCE)CC.1943-5614.0000204.

Bilotta, A., Di Ludovico, M., & Nigro, E. (2009a). Influence of effective bond length on FRP-concrete debonding under monotonic and cyclic actions, *Proceedings of the 9th International Symposium on Fiber Reinforced Polymer Reinforcement for Concrete Structures Sydney*, Australia 13–15 July 2009.

Bilotta, A., Ceroni, F., Di Ludovico, M., Fava, G., Ferracuti, B., Mazzotti, C., Nigro, E., Olivito, R., Pecce, M., Poggi, C. & Savoia, M. (2009b). Experimental round robin test on FRP concrete bonding, *Proceedings of FRP RCS9*, 13–15 July, Sydney, Australia, CD ROM.

Brosens, K., & Van Gemert, D. (1997). Anchoring stresses between concrete and carbon fibre reinforced laminates, *Proceedings of the 3rd International Symposium on Non-metallic (FRP) Reinforced for Concrete Structures*, (Vol. 1, October 1997, pp. 271–278).

Burdekin, F. M. (2007). General principles of the use of safety factors in design and assessment. *Engineering Failure Analysis, 14*(3), 420–433.

CEB-FIP (1993). Model Code 1990, Final Draft, Bulletin d'Information n. 213/214.

Ceroni, F., & Pecce, M. (2010). Evaluation of bond strength and anchorage systems in concrete elements strengthened with CFRP sheets, *Journal of Composites in Construction*, ASCE. (In press)

Chajes, M. J., Finch, W. W., Januszka, T. F., & Thomson, T. A. (1996). Bond and force transfer of composite material plates bonded to concrete, *ACI Structural Journal*, *93*(2), 208–217.

Chen, J. F., & Teng, J. G. (2001). Anchorage strength models for FRP and Steel Plates bonded to concrete. *ASCE Journal of Structural Engineering, 127*(7), 784–791.

CNR-DT 200. (2004). Guide for the design and construction of externally bonded FRP systems for strengthening, Council of National Research, Rome, http://www.cnr.it/documenti/norme/IstruzioniCNR_DT203_2006_eng.pdf.

Di Ludovico, M., Piscitelli, F., Prota, A., Lavorgna, M., Manfredi, G., & Mensitieri, G. (2009). CFRP Laminates Behavior at Elevated Temperature. In: *Proceedings of the 7th International Conference on Composite Science and Technology*, January 20–22, 2009, Sharjah, United Arab Emirates.

EN-1992, EC2. (2005). Design of concrete structures.

EN-1993, EC3. (2005). Design of steel structures.

EN-1994, EC4. (2004). Design of composite steel and concrete structures.

EN-1990, EC0. (1990). Basis of structural design.

European Commitee for Standardization. (2002). EN 1990-Eurocode: Basic of Structural Design.

European Commitee for Standardization. (2004). EN 1992–1-1-Eurocode 2: Design of Concrete Structures. Part 1-1: General Rules and Rules for Buildings, ENV 1992-1-1.

European Commitee for Standardization. (2005). EN 1998–3-Eurocode 8: Design of structures for earthquake resistance. Part 3: Assessment and retrofitting of buildings.

Faella, C., Martinelli, E., & Nigro, E. (2010). A simplified design formula for intermediate debonding failure in RC beams externally strengthened by FRP, 3rd fib International Congress, May 29—June 2, 2010, Paper ID: 672, 8, Washington, USA.

Faella, C., Martinelli, E., & Nigro, E. (2004). Debonding in FRP-strengthened RC beams: comparison between code provisions, *Proceedings of the 2nd International Conference on FRP Composites in Civil Engineering*, Paper 074, Adelaide (Australia), December 8–10, 2004.

Faella, C., Martinelli, E., & Nigro, E. (2008a). Direct versus Indirect Method for Identifying FRP-to-Concrete Interface Relationships. *Journal of Composites for Construction, 13*(3), 226–233.

Faella, C., Martinelli, E., & Nigro, E. (2008). Formulation and Validation of a Theoretical Model for Intermediate Debonding in FRP Strengthened RC Beams, Composites Part B 2008, (39(4), pp. 645–655).

Faella, C., Martinelli, E., Nigro, E., Salerno, N., Sabatino, M., & Mantegazza G. (2002). Aderenza tra calcestruzzo e fogli di FRP utilizzati come placcaggio di elementi inflessi.:Parte prima: risultati sperimentali, *Proceedings of* the *XIV C.T.E. Conference*, Mantova, Italy, Nov. 2002, (in Italian).

Faella, C., Martinelli, E., & Nigro, E. (2008). Some remarks on the parameters affecting debonding in FRP strengthened RC beams, *Proceedings of CICE 2008*, Zurich (CH), 22–24 July, Paper E 145.

Ferracuti, B., Martinelli, E., Nigro, E., & Savoia, M. (2007). Fracture Energy and Design Rules against FRP-Concrete Debonding, *Proceedings of 8th FRPRCS Conference*, 16–18 July 2007, Patras (GR).

fib. (2001). Externally Bonded FRP Reinforcement for RC Structures. fib Bulletin 14, Technical Report, Task Group 9.3—FRP Reinforcement for Concrete Structures, International Federation for Structural Concrete.

Grace, N. F., Sayed, G. A., Soliman, A. K., & Saleh, K. R. (1999). Strengthening Reinforced Concrete Beams Using Fiber Reinforced Polymer (FRP) Laminates. *ACI Structural Journal, 96*(5), 865–875.

JSCE. (2001). Recommendations for upgrading of concrete structures with use of continuous fiber sheets, Concrete Engineering Series 41.

Khomwan, N., Foster, S. J., & Smith, S. T. (2004). Debonding failure in CFRP strengthened concrete beams, *Proceedings of the 2nd International Conference on FRP Composites in Civil Engineering*, (pp. 505–514), CICE 2004, Adelaide (Australia).

Leone, M., Aiello, M. A., & Matthys, S. (2009). Effect of elevated service temperature on bond between FRP EBR systems and concrete. *Composites Part B: Engineering, 40*(1), 85–93.

Lu, X. Z., Teng, J. G., Ye, L. P., & Jiang, J. J. (2005). Bond–slip models for FRP sheets/plates bonded to concrete, Engineering Structures, (27, pp. 920–937) Elsevier.

Madsen, H. O., Krenk, S., & Lind, N. C. (1986). *Methods of structural safety*. Ellingwood Cliffs: Prentice-Hall.

Mazzotti, C., & Savoia, M. (2009). Experimental Tests on Intermediate Crack Debonding Failure in FRP—Strengthened RC Beams Advances in Structural Engineering (Vol. 12 No. 5).

Mazzotti, C., Savoia, M., & Ferracuti, B. (2008). An experimental study on delamination of FRP plates bonded to concrete. *Construction and Building Materials, 22*(7), 1409–1421.

Mazzotti, C., Savoia, M., & Ferracuti, B. (2009). A new single-shear set-up for stable debonding of FRP–concrete joints. *Construction and Building Materials, 23*(4), 1529–1537.

McSweeney, B. M., & Lopez, M. M. (2005). FRP-concrete bond behavior: a parametric study through pull-off testing. In C. K. Shield & J. P. Busel (Eds.), *Proceedings of 7th International Symposium FRP Reinforcement for Concrete Structures* (pp. 441–460). Kansas City, Missouri.

Melchers, R. E. (1987). Structural Reliability. Analysis and Prediction, John Wiley & Sons, New York, USA.

Monti, G., Alessandri, S., & Santini, S. (2009). Design by Testing: A Procedure for the Statistical Determination of Capacity Models, *Journal of Construction and Building Materials*, Special Issue on FRP Composites (Vol. 23, pp. 1487–1494), Elsevier.

Monti, G., & Petrone, F. (2014). Calibration of Capacity Models. *ASCE, Journal of Structural Engineering*, (submitted).

Mood, A. M., Graybill, F. A., & Boes, D. C. (1974). *Introduction to the Theory of Statistics* (3rd ed.). New York: McGraw-Hill.

Napoli, A., Matta, F., Martinelli, E., Nanni, A., & Realfonzo, R. (2010). Modelling and verification of response of RC slabs strengthened in flexure with mechanically fastened FRP laminates. *Magazine of Concrete Research, 62*(8), 593–605.

Neubauer, U., & Rostásy, F. S. (1997). Design aspects of concrete structures strengthened with externally bonded CFRP-plates, *Proceedings of 7th International Conference on Structural Faults and Repair Concrete + Composites* (Vol. 2, pp. 109–118).

Nigro, E., Di Ludovico, M., & Bilotta, A. (2008). FRP-concrete debonding: experimental tests under cyclic actions, *Proceedings of the 14th World Conference on Earthquake Engineering* . October 12–17, 2008, Beijing, China.

Pan, J., Chung, T. C. F., & Leung, C. K. Y. (2009). FRP Debonding from Concrete Beams under Various Load Uniformities Advances in Structural Engineering (Vol. 12 No. 6).

Pham, H., & Al-Mahaidi, R. (2004) Bond characteristics of CFRP fabrics bonded to concrete members using wet lay-up method, *Proceedings of the 2nd International Conference on FRP Composites in Civil Engineering*, CICE 2004 (pp. 407–412) Adelaide (Australia).

Said, H., & Wu, Z. (2008). Evaluating and proposing models of predicting IC Debonding Failure. *ASCE Journal of Composites for Construction, 12*(3), 284–299.

Sedlacek, G., & Kraus, O. (2007). Use of safety factors for the design of steel structures according to the Eurocodes. *Engineering Failure Analysis, 14*(3), 434–441.

Shapiro, S. S., & Wilk, M. B. (1965). An analysis of variance test for normality (complete samples). *Biometrika, 52*, 591–611.

Sharif, A., Al-Sulaimani, G. J., Basunbul, I. A., Baluch, M. H., & Ghaleb, B. N. (1991). Strengthening of Initially Loaded Reinforced Concrete Beams using FRP Plates. *ACI Structural Journal, 91*(2), 160–168.

Smith, S. T., & Teng, J. G. (2002). FRP-strengthened RC beams-I: review of debonding strength models. *Engineering Structures, 24*(4), 385–395.

Takeo, K., Matsushita, H., Makizumi, T., & Nagashima, G. (1997). Bond characteristics of CFRP sheets in the CFRP bonding technique. *Proceedings of Japan Concrete Institute, 19*(2), 1599–1604.

Taljsten, B. (1994). Plate bonding: Strengthening of existing concrete structures with epoxy bonded plates of steel or fibre reinforced plastics, Doctoral thesis, Lulea, University of Technology, Sweden.

Task Group 9.3. (2001). Externally Bonded FRP Reinforcement for RC Structures, Technical Report Bulletin 14, fib-CEB-FIP.

Teng, J. G., Chen, J. F., Smith, S. T., & Lam, L. (2001). FRP-strengthened RC structures (p. 245.) John Wiley and Sons: Chichester, West Sussex, UK.

Teng, J. G.; Lu, X. Z.; Ye, L. P., & Jiang, J. J. (2004). Recent Research on Intermediate Crack Induced Debonding in FRP Strengthened Beams, *Proceedings of the 4th International Conference on Advanced Composite Materials for Bridges and Structures*, Calgary, AB, Canada.

Teng, J. G., Smith, S. T., Yao, J., & Chen, J. F. (2003). Intermediate Crack Induced Debonding in RC Beams and Slabs. *Construction and Building Materials, 17*(6–7), 447–462.

Travassos, N., Ripper, T., & Appleton, J. (2005). Bond stresses characterization on CFRP-RC interfaces, *Proceedings of 3rd International Conference Composites in Construction*, CCC2005, Lyon, France.

Triantafillou, T., & Plevris, N. (1992). Strengthening of RC beams with epoxy-bonded FRP composite materials. *Materials and Structures, 25*, 201–211.

Ueda, T., Sato, Y., & Asano, Y. (1999). Experimental study on bond strength of continuous carbon fiber sheet, *Proceedings of 4th International Symposium on Fiber Reinforced Polymer reinforcement for Reinforced Concrete Structure* (pp. 407–16).

Wu, Z., & Niu, H. (2007). Prediction of Crack-Induced Debonding Failure in R/C Structures Flexurally Strengthened with Externally Bonded FRP Composite. *JSCE Journal of Materials, Concrete Structures and Pavements, 63*(4), 620–639.

Wu, Z. S., Yuan, H., Yoshizawa, H., & Kanakubo, T. (2001). Experimental/analytical study on interfacial fracture energy and fracture propagation along FRP-concrete interface, ACI International SP-201–8 (pp. 133–52).

Yao, J., Teng, J.G., & Chen, J.F. (2005). Experimental study on FRP-to-concrete bonded joints, Composites: Part B Engineering (Vol.36, pp. 99–113) Elsevier.

Yua, Z., Dinga, F., & Caib, C. S. (2007). Experimental behavior of circular concrete-filled steel tube stub columns. *Journal of Constructional Steel Research, 63*, 165–174.

Zhao, H. D., Zhang, Y., & Zhao, M. (2000). Research on the bond performance between CFRP plate and concrete, *Proceedings of 1st Conference on FRP Concrete Structures of China* (pp. 247–53).